OENO One
VINE AND WINE OPEN ACCESS JOURNAL
Volume 50 > Number 4 > 2016

Ultrastructural leaf features of grapevine cultivars (*Vitis vinifera* L. ssp. *vinifera*)

Christoph Konlechner and Ursula Sauer*

AIT Austrian Institute of Technology, Health & Environment Department, Bioresources, Konrad Lorenz Straße 24, 3430 Tulln, Austria. *corresponding author

Abstract

Aim: To investigate and compare *Vitis vinifera* Linné subsp. *vinifera* leaves of cultivars important for the Austrian wine producers in order to learn more about their surface architectures in the micro- and nanoscale.

Methods and results: Atomic force microscopy, binocular fluorescence microscopy, contact angle measurements, and environmental scanning electron microscopy were employed in order to assess physicochemical features of fresh plant material. Erect and prostrate trichomes are the most characteristic features present on the epidermal surfaces of grapevine leaves. These hairs occur in rather different densities from none to densely covering the whole surface. Contact angles are highly affected by these hairs, resulting in individual cases in values >150° in the presence of a high reclining hair density. On nanoscopic scale, blades of the varieties differ with respect to their wax structures in orientation, shape and size. Cuticular striae and epicuticular waxes, mostly granules and platelets, are conspicuous characteristics of grapevine leaf ultrastructure.

Conclusion: The microscopy techniques applied are complementary, enabling morphological analysis at different scales. They are not only efficient tools for descriptive botanics and for finding morphological adaptations to the environmental conditions, they provide also an insight into the habitat of leaf colonizing microbes, pathogenic as well as beneficial ones, and may add to the understanding of the conditions they find on leaf surfaces.

Significance and impact of the study: Leaf surface structures and chemicals are part of the defence system of the plant. Water-repellency can be advantageous for the plant as it creates unfavourable conditions for the successful colonization of pathogens. The knowledge of wetting properties of leaf surfaces will advance the insight in the interaction with additives, promoting the secure and optimal use of plant protection agents applied by spray deposition, especially under difficult weather conditions. The application of such research will be better contact and/or penetration, better adhesion of pesticides and other plant protecting agents, and improved adhesion of plant promoting bacteria in biocontrol applications.

Key words: epicuticular waxes, atomic force microscopy; contact angle; scanning electron microscopy

manuscript received 9th March 2016 - revised manuscript received 22 July 2016

*Corresponding author: ursula.sauer@ait.ac.at

OENO One, 2016, **50**, 4, 195 - 207

Introduction

The cuticle forms the multifunctional interface of plant and environment. Most prominently, it is a transpiration barrier, but it also controls leaf carbon balance, solute loss and uptake. Physiology, morphology and density of grapevine stomata have been investigated with respect to water stress (Costa *et al.,* 2012], soil temperatures and atmospheric carbon dioxide (Rogiers *et al.,* 2011] and wind (Gokbayrak *et al.,* 2008]. But leaf surfaces are also habitats for a great variety of different organisms, including lichens, bryophytes, algae, fungi, cyanobacteria, yeasts and other microorganisms as well as small animals (Ruinen 1961]. Bacteria are representing the biggest group among them. Highly important for agricultural species, the cuticle works as the first contact point and barrier against pathogenic fungi (Mendoza-Mendoza *et al.,* 2009], viruses (Khan *et al.,* 2011], and bacteria (Marcell and Beattie, 2002], and it is responsible for host recognition by fungi as well as herbivorous insects (Powell *et al.,* 1999] and their predators. Adhesion of bacteria and fungal spores relates to the physicochemical features of the cuticle and hence investigations of these are a highly significant topic for agricultural research. Thickness, structure and chemical composition of cuticular matrices and epicuticular and intracuticular waxes vary widely (Riederer and Schreiber, 2001; Koch *et al.,* 2004]. The different shapes of the wax crystals are determined by their chemistry, i.e., certain crystal types are formed by specific compounds (Koch *et al.,* 2006]. Barthlott *et al.,* [1998] identified 23 types of epicuticular wax deposits and assigned to them high systematic significance mainly for higher taxonomic levels. The potential functional consequences of such differences are still poorly understood (Kerstiens 2010]. Fungal spores usually need free water or a relative humidity of 95% to germinate. Many fungi infect leaves via an infection drop - a drop of rainwater or dew (Blakeman 1973]. Thus water-repellency is advantageous for the plant as it creates unfavourable conditions for the successful colonization of pathogens and parasitic fungi (Bargel *et al.,* 2006]. Some pathogens are able to overcome the barrier of a leaf covered with epicuticular wax structures making it highly hydrophobic. Powdery mildews, for example, contain a small amount of water within their conidia which enables them to germinate on virtually dry surfaces (Barthlott and Neinhuis 1997]. Monteiro *et al.,* [2013] and Santos *et al.,* [2014] studied epidermis, stomata, hair distribution and mesophyll structure, finding significant differences between four red and four white grapevine cultivars from Portugal. Investigations on the impact of such differences on physiological behaviour and susceptibility are still in progress. Boso *et al.,* [2010] for instance found no evidence of a link between hair density and susceptibility to grapevine downy mildew in six different grapevine varieties.

Interestingly, the ultrastructure and the related wetting behaviour of plant surfaces has been studied intensely for a long time due to their role in pesticide spray deposition, adhesion of leaf fertilizers and application of spray additives (e.g. Watanabe and Yamaguchi 1991, Smith *et al.,* 2000]. An early report on wetting of leaves was published in *Pesticide Science* (Holloway 1970], with a focus on the penetration of leaves by spray chemicals, identifying *exposed chemical groups and surface roughness* as the main factors.

Few publications such as Bensalem-Fnayou *et al.,* [2009] or Boso *et al.,* [2011] describe microscopic examination of grapevine leaves using SEM and AFM techniques, while there is quite a number of reports on ultrastructural investigations of grape berries. Grapevine as a highly economic crop with its enormous pesticide consumption is predestined to be examined with these tools, thus it seems contradictory that barely no evidence about the surface ultrastructure of leaves of *Vitis vinifera* varieties exists. In order to start closing this gap, surface architectures of leaves of 18 cultivars of *Vitis vinifera* Linné subsp. *vinifera* were subject of investigation herein. Samples represented the most commonly grown grapevine varieties in Austria, covering 88% of the Austrian yield area. Atomic force microscopy, binocular fluorescence microscopy, contact angle measurements, and environmental scanning electron microscopy were employed in order to assess physicochemical features of fresh plant material.

Material and Methods

All grapevine leaf samples were taken from the 8th or 9th node of this year grown shoots in order to use fully mature leaves. The grapevine leaves were stored at 4 °C air-sealed in plastic bags until assessment. Most varieties were sampled at a research garden of the University of Natural Resources and Life Sciences in Tulln, Austria. Chasselas rouge (Rote Gutedel), Riesling, Welschriesling and Veltliner grün were kindly provided by Weinbau Carl-Friedrich Bacher, Tulln, Austria. Vines were treated with Netzschwefel (Agrostulln, D), Curifol WG (Kwizda Agro, A), Prosper (Bayer, A), and Karathane Gold

(Dow AgroSciences, D). Samples were taken at least a fortnight after fungicide treatment.

1. Binocular fluorescence microscopy

Samples were investigated with the binocular fluorescence microscope Olympus SZX16 on the adaxial and abaxial surface. Fresh leaves were investigated without specimen preparation. The ET bandpass filter 525/50 Chroma was used to observe samples (γ=550-500 nm).

2. Atomic force microscopy (AFM)

For AFM measurements with NanoWizard (II) AFM from JPK instruments (Germany), about 2.5 x 1.5 cm areas of the leaves were excised with a scalpel. All leaves were fixed with a two-component epoxy adhesive on a microscope slide. Adaxial sides desiccated at least 1.5 to 2 hours before scanning in order to avoid drift of the cantilever due to the humidity of the leaves when approaching to the sample. Abaxial side scans were dried overnight at room temperature. Intermittent Contact Mode in air was chosen using NSC35/AIBS cantilever-chip (radius of tip curvature <10 nm) from µMasch (Bulgaria). While the adaxial side of each sample was scanned, abaxial surfaces were only imaged if the variety did display a very low density of reclining hairs, as assessed with fluorescence microscopy. Scan rate was 0.3 lines per second. Common z-range was 15 µm, however, for some small area scans a diminished z-range of 12 µm or 5.58 µm was used. Images were evaluated and edited with JPK Data Processing software (Version spm-4.2.62).

3. Environmental scanning electron microscopy (ESEM)

Leaf parts were excised with an 8-mm stamper between secondary veins and observed without further specimen preparation in the ESEM. The samples were frozen and fixed with a cooling stage at -25 °C in the specimen chamber directly. Hitachi TM3030 device (Hitachi, Germany) was used for the ESEM using 15 kV accelerating voltage. Both abaxial and adaxial surfaces were investigated with ESEM.

4. Contact angle measurements

The contact angles of the water drop on the adaxial and abaxial surface were measured with a goniometer (CAM 101 device form KSV, Finland) and determined with Attension Theta Software (Version 4.1.9.8). Before the measurements leaves were briefly rinsed with dH_2O. The samples were taken from the leaf-base, middle part and leaf-head, avoiding bigger leaf veins (veins of the first or second order). Leaves were put as flat as possible on the device without any adhesive and/or supportive material and 6 µL of sterile H_2O was pipetted on it. 18 replicate measurements per leaf side were performed and mean values and standard deviations calculated.

Results and Discussion

1. Binocular fluorescence microscopy

Grapevine trichomes, so called prostrate and erect hairs, were found to be characteristic features of the varieties. Due to autofluorescence their presence and density could be easily assessed with fluorescence microscopy. All adaxial leaf surfaces exhibited no or a very low density of reclining hairs. The abaxial surfaces however were found to differ distinctively with respect to both prostrate and erect hair density. Erect hairs, which are spine like trichomes, mainly rose from leaf veins and appeared to be very characteristic of each genotype ranging from complete absence (Müller-Thurgau, Pinot blanc, Chardonnay blanc) to dense coverage (e.g. Riesling). In Figure 1, examples of erect trichomes are shown on two grapevine varieties, Pinot noir (mainly in the vein axil) and Blaufränkisch. A close up on prostrate and erect grapevine trichomes observed with binocular fluorescence microscopy is shown in Figure 2; curled and spiky structures of the two varieties are clearly visible. In Table 1, occurrence of the two types of hairs and their density are listed for all cultivars, assigning the descriptors for hair density according to the Organisation Internationale de la Vigne et du Vin (OIV Descriptor List, 2nd edition 2001]: 1 = none or very low, 3 = low, 5 = medium, 7 = high, 9 = very high.

Boso *et al.,* [2011] claimed that the trichomes of grapevine are characteristic features for each genotype, and that reclining trichomes consist of β-1,3-glucans, the main one being callose, an unbranched 1,3-β-D-glucose (Stasinopoulos *et al.,* 1999]. We could support this by staining reclining hairs with aniline blue, a substance known for mainly targeting β-1,3-glucans (Diez-Navajas *et al.,* 2007]. As callose synthesis is suggested to be guaranteed by dedicated enzymes, which are regulated over a plurality of genes (Verma and Hong 2001], it is possible that the genetic background leads to the fact that *V. vinifera* varieties are able to synthetize callose in different amounts and/or for different reasons. Callose was either found to be synthetized throughout growth or formed due to biotic and abiotic stress (Stone and Clarke 1992]. Incidence of prostrate hairs may hence also depend on environmental factors and

OENO One, 2016, **50**, 4, 195 - 207

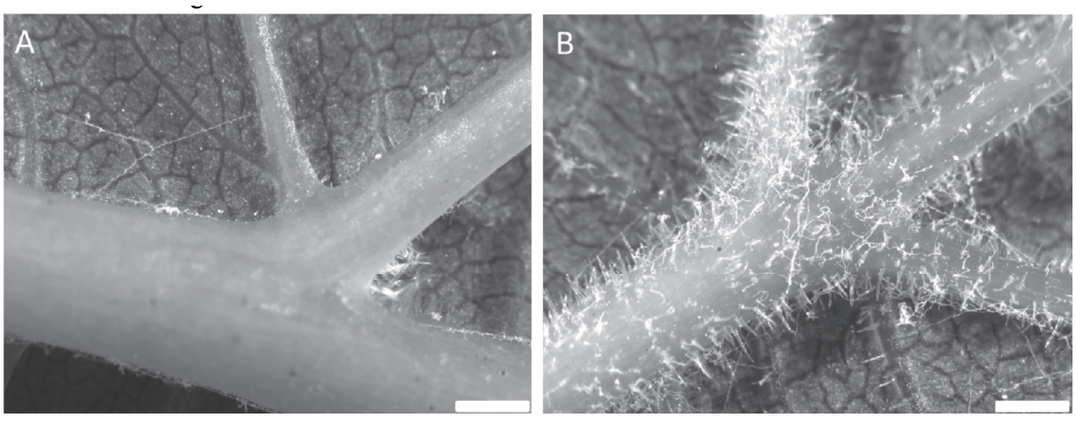

Figure 1 - Binocular Fluorescence Microscopy with γ=550-500 nm filter; (A) Pinot noir abaxial surface with a major leaf vein with scarce erect hairs in contrast to (B) the major leaf vein of Blaufränkisch abaxial surface, densely covered with erect trichomes and a few reclining hairs. Scale bars: 1 mm

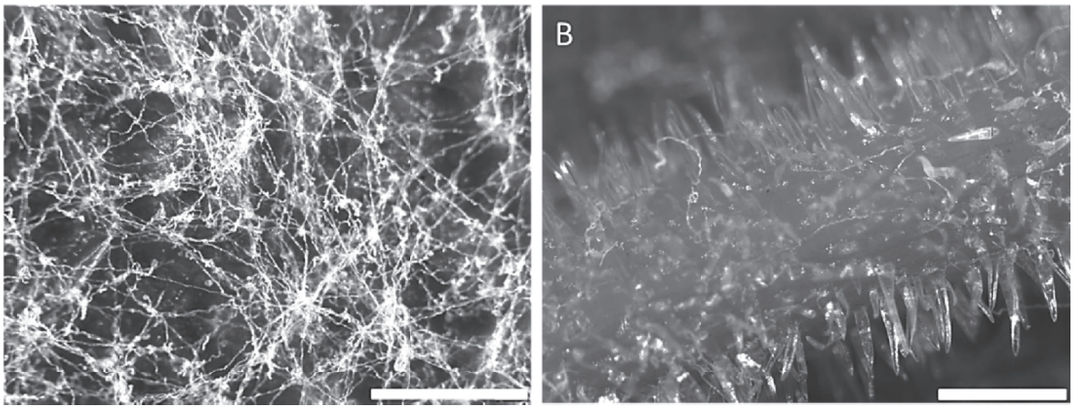

Figure 2 - Binocular Fluorescence Microscopy with γ=550-500 nm filter. Abaxial surfaces of (A) Veltliner grün with dense coverage of reclining hair and of (B) Zweigeltrebe blau reclining with high density of erect hair on a vein. Scale bars: 1 mm

growth period. Reclining hair formation being presumably dependent on external factors was already shown by Palliotti *et al.,* [2000] when investigating effects of light and shadow conditions on grapevine leaves. Gindro *et al.,* [2003] even considered callose formations and depositions to be associated with systemic acquired resistance (SAR) and could prevent secondary infections with fungi of non-infected stomata.

2. Atomic force microscopy (AFM)

All white genotypes showed epicuticular wax depositions in the form of platelets, granules or even plates; Chardonnay additionally displayed fissured layers of wax (Figure 3). The smallest wax structures were observed in Chasselas rouge, a mutation of Chasselas blanc, on the abaxial side with sizes reaching from just 50 nm to about 500 nm. Even stomata were covered with these wax platelets. Pinot blanc, on the other hand, had dense layers of platelets and plates, reaching up to 3 mm in diameter. None of the white varieties showed as pronounced cuticular striae on the adaxial sides as the red varieties did (see Figures 4 and 5). Most red ones featured conspicuous cuticular striae on their cells' surfaces. Especially on nerves of Merlot noir and Regent they appeared more parallel, while Zweigeltrebe blau and Portugieser blau had strongly curled striae. The density of wax granules and platelets sitting on these adaxial striae varied from extremely dense (Wildbacher blau, Fig. 4 (G) and (H)) to quite low (Blauburger Fig. 4 (E) and (F)). On Blauburger, fungal hyphae were found on the fresh leaf.

The shape and size of epicuticular waxes is summarized in Table 1. As about 50% of the varieties could not be scanned on the abaxial side due to trichomes, this structural information is available only for some genotypes. The vast majority of all

Table 1 - List of features of the examined grapevine varieties; characteristics of the grapevine epicuticular waxes based on the AFM scans; wax size complies with a rough average of the wax depositions measured on the AFM detail scans, adaxial side (ad) and abaxial side (ab); SD = standard deviation, hair density: 1 = none or very low, 3 = low, 5 = medium, 7 = high, 9 = very high.

Variety		Side	Wax density	Wax shape	Wax size [nm]	Density of erect hairs	Density of reclining hairs	Contact angle [°]± SD
Veltliner grün	white	ad	medium	granules/platelets	400-1500	1- none	3- low	62 ± 14
		ab	n.a.	n.a.		1- very low	9- very high	152 ± 08
Welschriesling	white	ad	high	granules	200-900	1- none	1- very low	104 ± 17
		ab	n.a.	n.a.		5- medium	7- high	145 ± 12
Müller-Thurgau	white	ad	high	granules	400-800	1- none	1- none	90 ± 10
		ab	high	granules/platelets	600-1500	1- none	1- very low	111 ± 11
Pinot blanc	white	ad	high	platelets	1500-3000	1- none	1- none	96 ± 07
		ab	high	granules	200-500	1- none	1- very low	105 ± 25
Riesling	white	ad	high	granules	200-400	1- none	1- very low	125 ± 16
		ab	n.a.	n.a.		7- high	7- high	133 ± 14
Chardonnay blanc	white	ad	high	fissured layers	2000-4000	1- none	1- very low	103 ± 10
		ab	medium	granules/platelets	150-900	1- none	1- very low	119 ± 16
Sauvignon blanc	white	ad	medium	granules/platelets	400-1000	1- very low	1- very low	98 ± 14
		ab	n.a.	n.a.		5- medium	7- high	143 ± 12
Chasselas rouge	rose	ad	medium	granules	150-900	1- none	1- none	81 ± 20
		ab	high	platelets	50-500	3- low	1- very low	59 ± 19
Zweigeltrebe blau	red	ad	low	granules/platelets	400-900	1- very low	1- very low	71 ± 17
		ab	n.a.	n.a.		7- high	3- low	111 ± 12
Blaufränkisch	red	ad	low	granules	200-600	1- none	1- very low	86 ± 11
		ab	high	platelets	500-1500	5- medium	3- low	117 ± 12
Portugieser blau	red	ad	medium	granules	300-1000	1- none	1- none	95 ± 15
		ab	n.a.	n.a.		1- none	1- very low	101 ± 08
Blauburger	red	ad	medium	granules/platelets	800-1500	1- none	1- very low	98 ± 09
		ab	n.a.	n.a.		3- low	1- very low	116 ± 19
Saint Laurent	red	ad	high	platelets	400-2000	1- none	1- none	98 ± 13
		ab	n.a.	n.a.		1- none	1- very low	126 ± 09
Pinot noir	red	ad	low	granules	400-800	1- none	1- very low	96 ± 07
		ab	n.a.	n.a.		1- very low	1- very low	105 ± 25
Merlot noir	red	ad	medium	platelets	300-1500	1- none	1- very low	118 ± 09
		ab	n.a.	n.a.		3- low	5- medium	135 ± 13
Wildbacher blau	red	ad	high	granules/platelets	300-1000	1- none	3- low	124 ± 08
		ab	n.a.	n.a.		1- none	5- medium	140 ± 09
Roesler	red	ad	medium	platelets	800-3000	1- none	1- none	108 ± 11
		ab	n.a.	n.a.		1- very low	7- high	136 ± 10
Regent	red	ad	high	granules/platelets	200-1500	1- none	1- none	90 ± 11
		ab	high	granules/platelets	100-900	1- very low	1- very low	107 ± 14

OENO One, 2016, **50**, 4, 195 - 207

varieties featured epicuticular waxes in the form of granules or platelets.

The AFM scans provided detailed structural information of the most common Austrian grapevine varieties. Overview scans (50 x 50 µm) showed the cell shapes, although in a limited area. The high resolution scans in small areas are thus of more interest when using AFM, leaving the overview observation to ESEM. These small area scans (10 x 10 µm) primarily revealed the structures of epicuticular wax depositions and larger cell surface structures as cuticular folds, so-called striae.

AFM has been applied in a few studies on the nanostructures of leaf surfaces providing quantitative

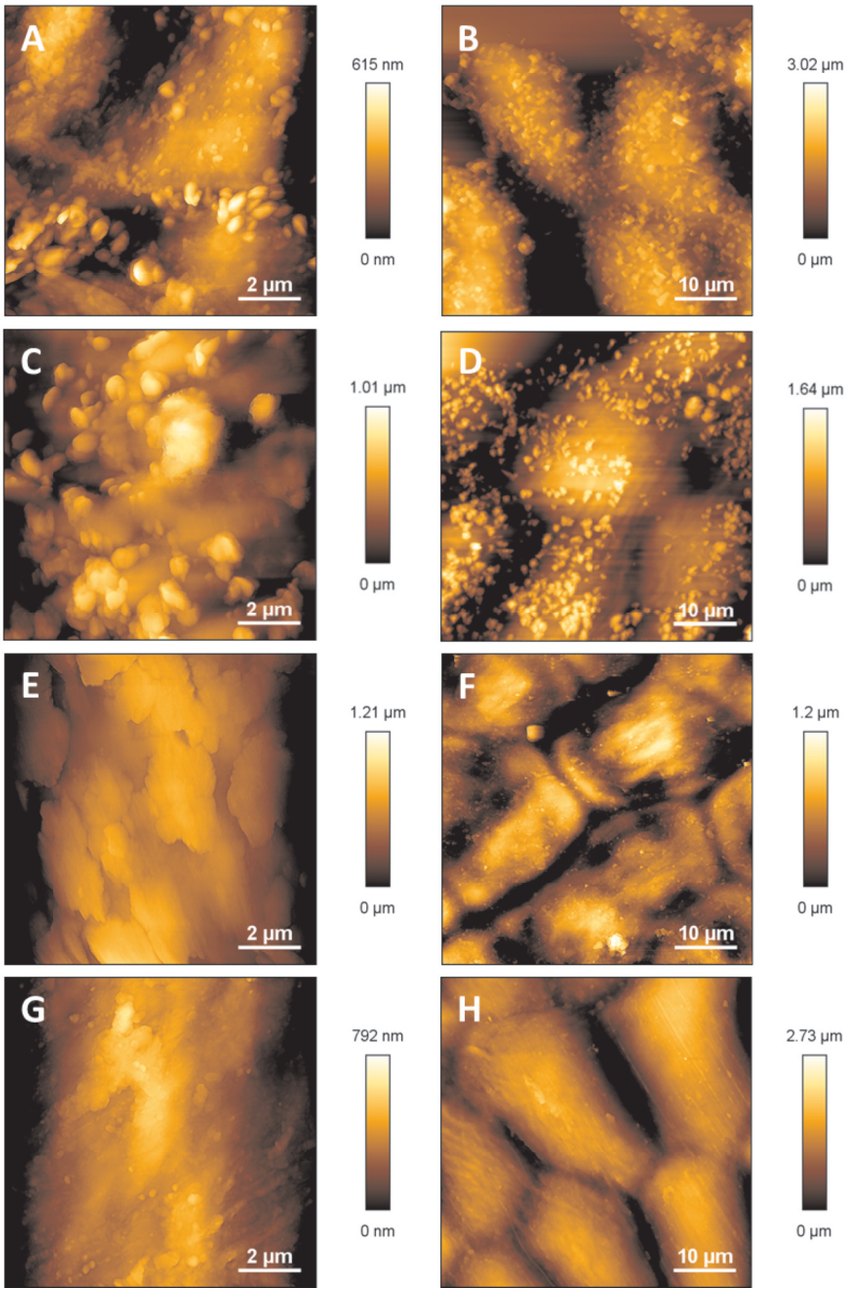

Figure 3 - AFM height images of grapevine leaves, adaxial: white varieties (A) Veltliner grün, wax platelets and granules; (B) Welschriesling; (C) Müller-Thurgau, dense platelets and granules; (D) Pinot blanc, granules; (E) Chardonnay, fissured wax layers; (F) Riesling, tiny granules; (G) Sauvignon blanc, granules; (H) Chasselas rouge, cuticular striae with granules.

information on leaf topography at the micro- and nanoscale. Mechaber *et al.,* [1996] were the first to use AFM for recording leaf texture, finding striking differences in roughness of young and old leaves of *Vaccinium macrocarpum*. Bargel *et al.,* [2006] imaged molecular steps on the surface of single wax crystals with AFM; such steps are virtually undetectable by SEM. And in Koch *et al.,* [2004], wax crystal formation on leaves of various species at the molecular level was shown for the first time with an AFM time-series under environmental conditions *in vivo*.

Less attention has been paid to the understanding of the functional aspects of these structures for the plants themselves (reviewed by Bargel *et al.,* 2006] and their relation to the habitat. Thinking of the leaf surface as a habitat for e.g. microbes, these small

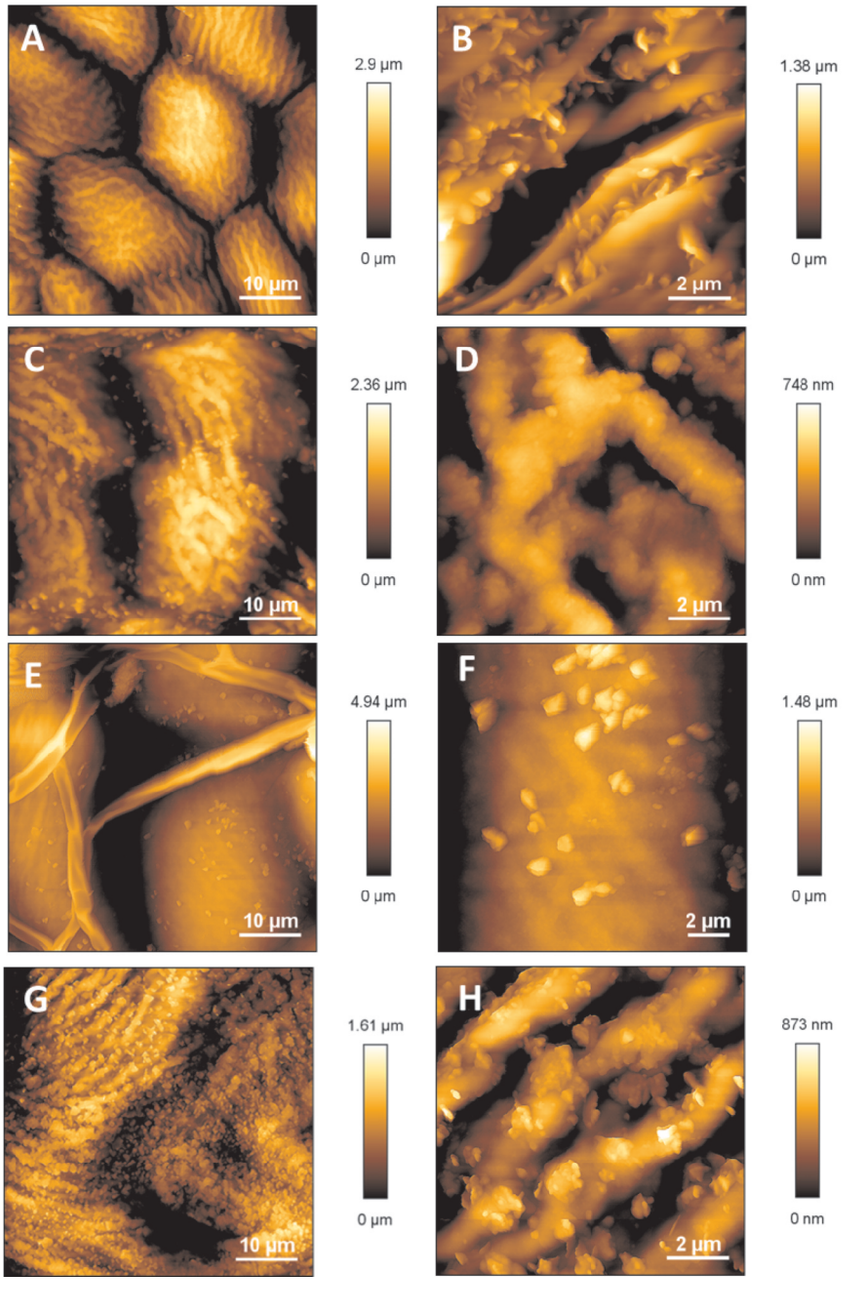

Figure 4 - AFM height images of the adaxial surface of red varieties showing a scan area of 50 x 50 µm (left) and 10 x 10 µm (right): (A) Zweigeltrebe blau, curled cuticular folds, and (B) Zweigeltrebe blau platelets; (C) Portugieser blau, cuticular striae and (D) Blauer Portugieser, granules; (E) Blauburger with fungal hyphae and (F) Blauburger platelets; (G) Wildbacher blau, cuticular folds and (H) Wildbacher blau, dense granules.

OENO One, 2016, **50**, 4, 195 - 207

structures together with the trichomes form the landscape they encounter (Vacher *et al.,* 2016].

3. Environmental scanning electron microscopy (ESEM)

The ESEM observations especially revealed structures over larger areas such as cell shapes, distribution of stomata and densities of reclining and erect trichomes on the adaxial and abaxial surfaces. Cell shape of the adaxial leaf surface of red and white varieties was polygonal and on small leaf veins more elongated or even rectangular. The abaxial surfaces revealed more morphological differences especially with respect to erect and prostrate hairs, as shown in Figure 5 for the white grapevine genotypes and in Figure 6 for red ones. Stomata were only found on the abaxial surface of all examined grapevine leaves, hypostomatic leaves being a characteristic feature of *Vitis vinifera* (Boso *et al.,* 2011].

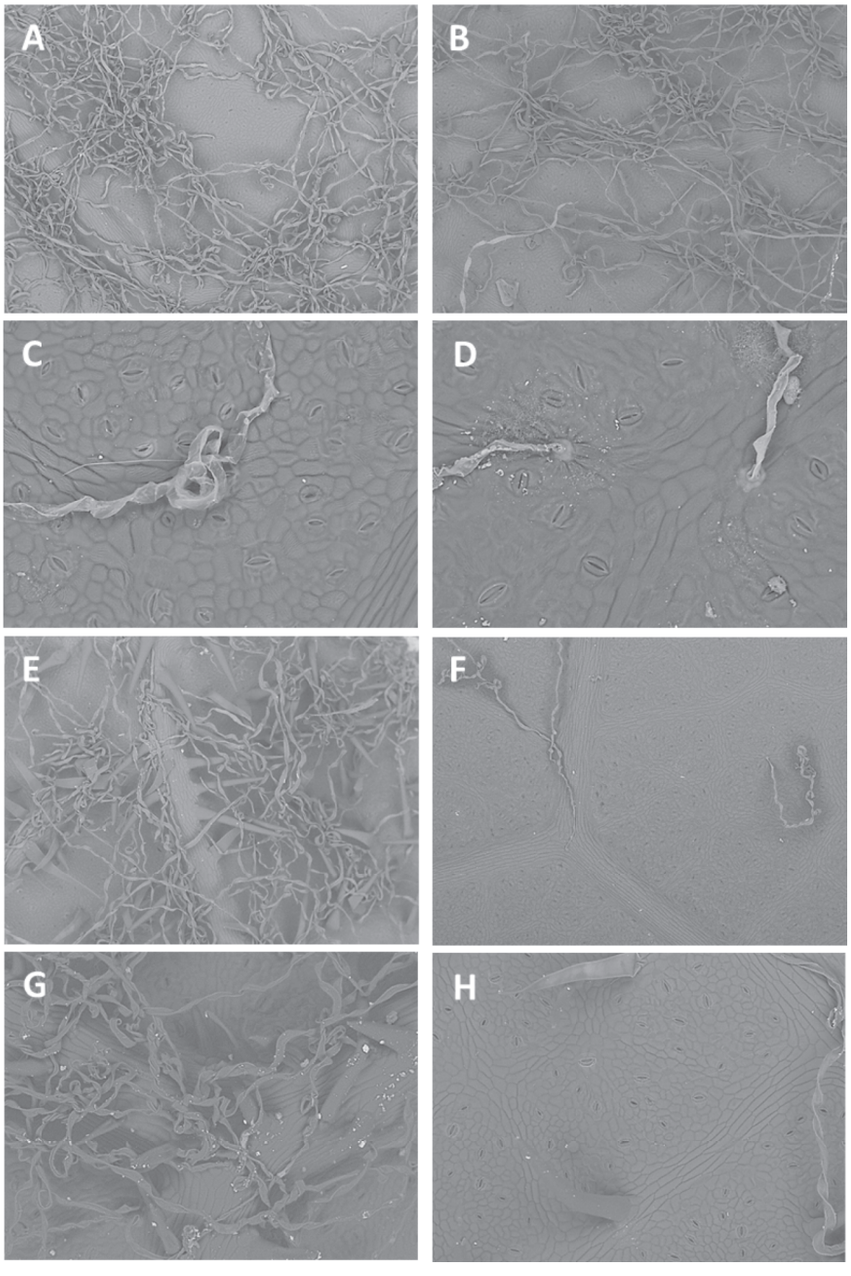

Figure 5 - ESEM images of grapevine leaves, abaxial: white varieties (A) Veltliner grün, x100; (B) Welschriesling, x100; (C) Müller-Thurgau, x500; (D) Pinot blanc, x500; (E) Riesling, x100; (F) Chardonnay, x100; (G) Sauvignon blanc, x250; (H) Chasselas rouge, x250.

For the white varieties reclining hairs were missing or extremely scarce on Chardonnay blanc, Chasselas rouge, Müller-Thurgau, and Pinot blanc. Erect trichomes were found very distinctively on Riesling, strongly surrounded with reclining hairs, and on Chasselas rouge (Figure 5).

The abaxial surface of Veltliner grün is covered in dense, curled prostrate trichomes, while Chasselas rouge shows some erect ones, allowing a look directly onto the leaf surface. In combination with binocular fluorescence microscopy the presence and density of the trichomes on the abaxial surfaces could be assessed easily (Table 1).

Features apart from trichomes became evident in the form of the density of the stomata, the mean number of stomata per mm² being 170 and 180 for white and red varieties, respectively. Only Müller-Thurgau and

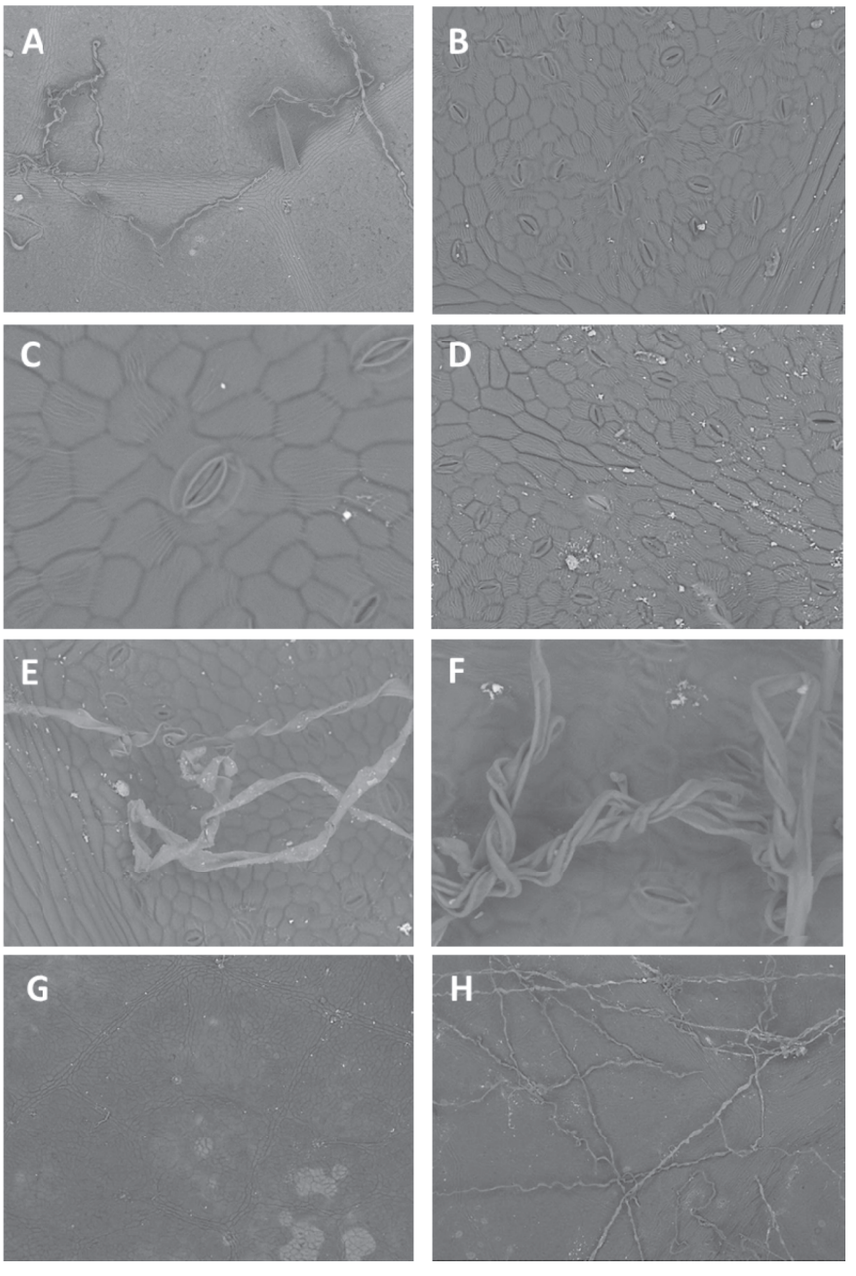

Figure 6 - ESEM images of grapevine leaves, abaxial: red varieties (A) Zweigeltrebe blau, x100; (B) Portugieser blau, x500; (C) Blaufränkisch, x1000; (D) Blauburger, x500; (E) St Laurent, x500; (F) Merlot, x1000; (G) Wildbacher blau, x100; (H) Roesler, x100.

OENO One, 2016, **50**, 4, 195 - 207

Portugieser blau were standing out with 290 and 230 stomata per mm².

Images in Figure 7 are close-up ESEM observation of grapevine leaves, highlighting distinct structures as well as bacteria and fungi colonizing them.

4. Contact angle measurements in relation to structural features

Despite the sensitivity of the method and the high variability expected for fresh leaf material, reproducibility of the measurements was adequate, indicated by an average coefficient of variation of 13%.

The contact angle measurements resulted in distinctive differences for the varieties (see Table 1 and Figure 8). The lowest mean contact angles (CAs) on both leaf sides were observed in Chasselas rouge

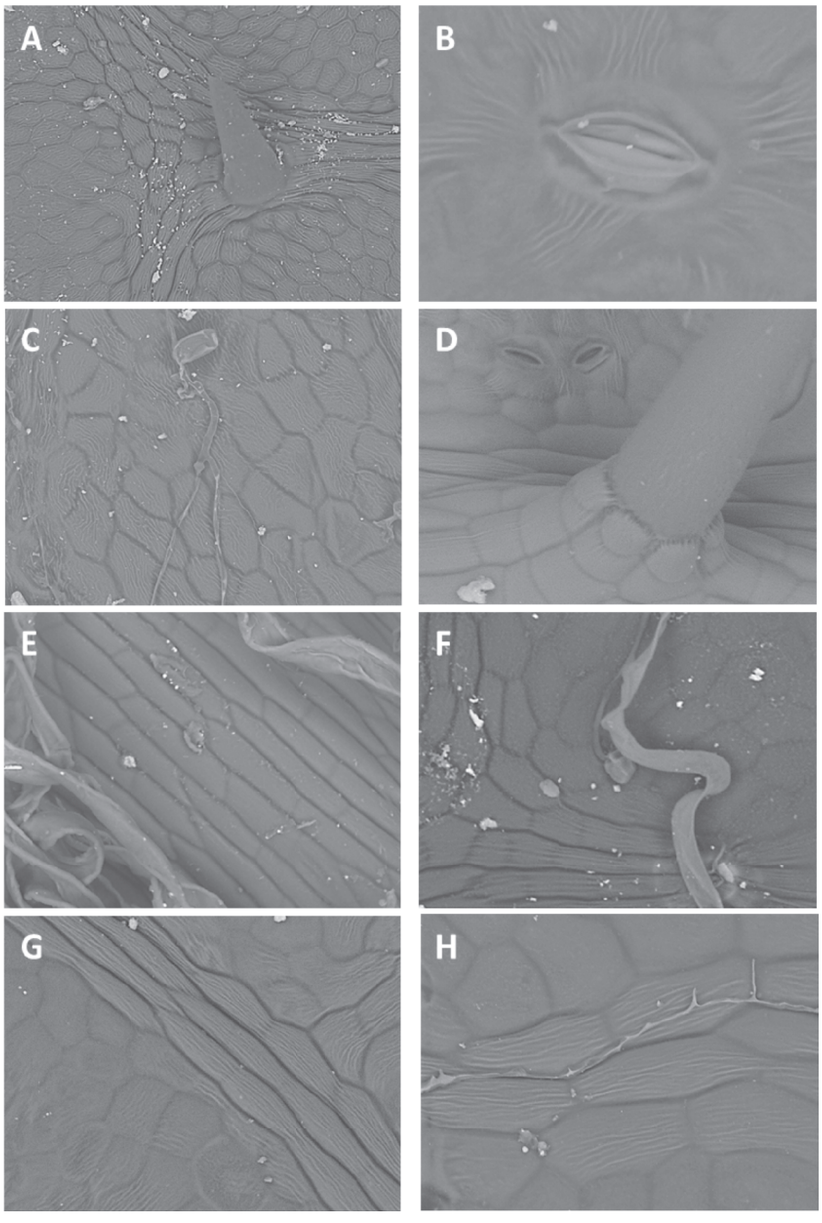

Figure 7 - ESEM images -(A) Müller-Thurgau, adaxial, erect hair protruding from a vein, microbes x500; (B) Stoma on Wildbacher blau, x2500 µm; (C) Blauburger with conidia, hyphae and microbes, and (D) Zweigeltrebe blau, anchorage of an erect trichome, x1000; (E) Riesling, vein on abaxial surface and prostrate trichomes, x1000; (F) Pinot noir adaxial surface, showing a fungal spore just forming a hyphae beside a reclining hair, x1000; (G) hairless adaxial blade of Regent with parallel cuticular striae, x1000; (H) Fungal hypha with appressoria tracing the shape of epidermal cells and cuticular striae, x1000.

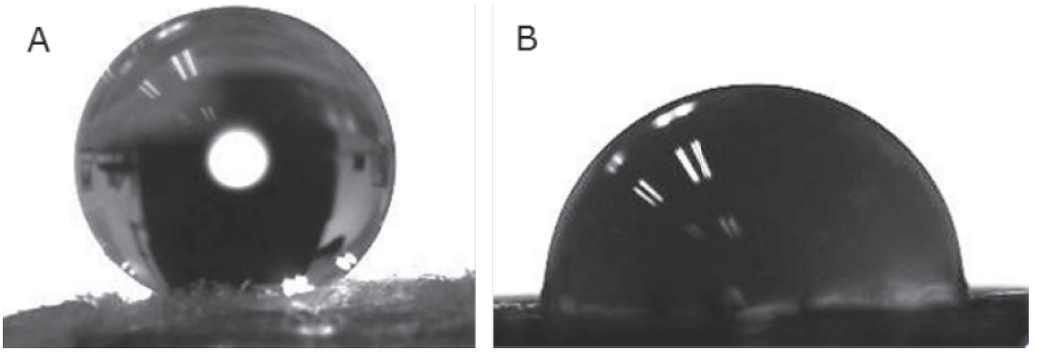

Figure 8 - (A) A drop of 6 µL dH_2O water forms almost spherical drop on the abaxial surface of a Veltliner grün leaf; Veltliner grün displayed the highest CAs on the abaxial surface among all examined varieties with single contact angles >160° (average: 152 ± 8°), indicating extreme hydrophobic surface structures; (B) in contrast, a water drop on a Saint Laurent adaxial side at the leaf base featuring CAs around 90°.

(81° adaxial and 59° abaxial) despite a high wax density. Remarkably hydrophobic abaxial leaves were found in the varieties Veltliner grün (152 ± 8°), Welschriesling (145 ± 12°), Sauvignon blanc (143 ± 12°) and Wildbacher blau (140 ± 9°).

For only three out of 18 tested varieties ad- and abaxial contact angles were not significantly different. Pinot noir and Portugieser blau, varieties with very low or absent hair-growth, showed low hydrophobicity on both leaf sides (96 ± 7° and 105 ± 25°; 95 ± 15° and 101 ± 8°, respectively). Riesling showed high contact angles on the adaxial side (125 ± 16°), not much different from the abaxial side densely covered with trichomes (133 ± 14°). For all other cultivars the difference between ad- and abaxial side was significant (t-test, α=0.01), ranging between 12 and 59%.

Density of reclining hair was positively correlated with high contact angles: all varieties with high or very high density featured contact angles above 135° (Veltliner grün, Riesling, Welschriesling, Sauvignon blanc, Merlot, Roesler and Wildbacher). Absent or very low hair density on the other hand was not always linked to low contact angles. The adaxial sides of Riesling and Wildbacher for instance feature high contact angles despite the absence of both trichome types. Here the high density of small wax granules and dense cuticular folds (Wildbacher) might explain the hydrophobic behaviour.

Conclusions

The microscopy techniques applied herein are complementary, enabling morphological analysis at different scales. Environmental scanning electron microscopy and binocular fluorescence microscopy have been shown to be excellent tools for fast and simple assessment of micromorphological characteristics of grapevine leaves with no or minimal sample preparation needed. Atomic force microscopy on the other hand allows insights in the ultrastructure of leaves, revealing the organization of epicuticular waxes in the micro- and nanoscale. They are not only efficient tools for descriptive botanics and for finding morphological adaptations to environmental conditions, they provide also an insight into the habitat of leaf colonizing microbes, pathogenic as well as beneficial ones, and may add to the understanding of the conditions epiphytes find on leaf surfaces.

Using leaves of the same developmental stage, we excluded leaf age as a factor, still weather conditions, microclimate, sun and shadow leaves may account for some of the differences observed between grapevine varieties. Water stress for instance has been reported to cause changes in grapevine morphology and anatomy (Costa *et al.,* 2012, Monteiro *et al.,* 2013].

Knowledge on the ultrastructural and chemical features of the plant as well as wetting properties of plant surfaces as specified by the water contact angle will have great impact on agricultural research. Firstly, leaf surface structures and chemicals are part of the defence system of the plant, related to e.g. crop-pathogen interactions and defence of herbivores. Second, the application of such research is better contact or penetration of pesticides and other plant protecting agents and improved adhesion of plant promoting bacteria in biocontrol applications.

Acknowledgements : We thank Weinbau Carl-Friedrich Bacher, Günther Brader (AIT), Michaela Griesser (University of Natural Resources and Life Sciences) and

Helga Reisenzein (AGES) for grapevine samples, and Land Niederösterreich for funding.

References

Bargel H., Koch K., Cerman Z., Neinhuis C., 2006. Structure-function relationships of the plant cuticle and cuticular waxes - a smart material? *Functional Plant Biology*, **33**, 893-910.

Barthlott W., Neinhuis C., 1997. Purity of the sacred lotus, or escape from contamination in biological surfaces. *Planta*, **202**, 1-8.

Barthlott W., Neinhuis C., Cutler D., Ditsch F., Meusel I., Theisen I., Wilhelmi H., 1998. Classification and terminology of plant epicuticular waxes. *Botanical Journal of the Linnean Society*, **126**, 237-260.

Bensalem-Fnayou A., Jellouli N., Bouamama B., Mliki A., Ghorbel A., 2009. Investigations on the leaf surface ultrastructure in grapevine (*Vitis vinifera* L.) by scanning microscopy. *Scanning*, **31**, 127-131.

Blakeman P.J., 1973. The chemical environment of leaf surfaces with special reference to spore germination of pathogenic fungi. *Pesticide Science*, **4**, 575-588.

Boso S., Alonso-Villaverde V., Santiago J.L., Gago P., Dürrenberger M., Düggelin M., Kassemeyer H.H., Martinez M.C., 2010. Macro- and microscopic leaf characteristics of six grapevine genotypes (*Vitis* spp.) with different susceptibilities to grapevine downy mildew. *Vitis*, **49**, 43-50.

Boso S., Gago P., Alonso-Villaverde V., Santiago J.L., Mendez J., Pazos I., Martínez M.C., 2011. Variability at the electron microscopic level in leaves of members of the genus *Vitis*. *Scientia Horticulturae*, **128**, 228-238.

Costa J.M., Ortuno M.F., Lopes C.M., Chaves M.M., 2012. Grapevine varieties exhibiting differences in stomatal response to water deficit. *Functional Plant Biology*, **39**, 179-189.

Díez-Navajas A.M., Greif C., Poutaraud A., Merdinoglu D., 2007. Two simplified fluorescent staining techniques to observe infection structures of the oomycete *Plasmopara viticola* in grapevine leaf tissues. *Micron*, **38**, 680-683.

Gindro K., Pezet R., Viret O., 2003. Histological study of the responses of two *Vitis vinifera* cultivars (resistant and susceptible) to *Plasmopara viticola* infections. *Plant Physiology and Biochemistry*, **41**, 846-853.

Gokbayrak Z., Dardeniz A., Bal M., 2008. Stomatal density adaptation of grapevine to windy conditions. *Trakia Journal of Science*, **6**, 18-22.

Holloway P.J., 1970. Surface factors affecting the wetting of leaves. *Pesticide Science*, **1**, 156-163.

Kerstiens G., 2010. Plant Cuticle. eLS. John Wiley and Sons, New York.

Khan M.A.U., Shahid A.A., Rao A.Q., Kiani S., Ashraf M.A., Muzaffar A., Husnain T., 2011. Role of epicuticular waxes in the susceptibility of cotton leaf curl virus (CLCuV). *African Journal of Biotechnology*, **10**, 17868-17874.

Koch K., Neinhuis C., Ensikat H-J., Barthlott W., 2004. Self assembly of epicuticular waxes on living plant surfaces imaged by atomic force microscopy (AFM). *Journal of Experimental Botany*, **55**, 711-718.

Koch K., Dommisse A., Barthlott W., 2006. Chemistry and crystal growth of plant wax tubules of Lotus (*Nelumbo nucifera*) and Nasturtium (*Tropaeolum majus*) leaves on technical substrates. *Crystal Growth & Design*, **6**, 2571-2578.

Marcell L.M., Beattie G.A., 2002. Effect of leaf surface waxes on leaf colonization by *Pantoea agglomerans* and *Clavibacter michiganensis*. *MPMI*, **15**, 1236-1244.

Mechaber W.L., Marshall D.B., Mechaber R.A., Jobe R.T., Chew F.S., 1996. Mapping leaf surface landscapes. *PNAS*, **93**, 4600-4603.

Mendoza-Mendoza A., Berndt P., Djamei A., Weise C., Linne U., Marahiel M., Vranes M., Kämper J., Kahmann R., 2009. Physical-chemical plant-derived signals induce differentiation in *Ustilago maydis*. *Molecular Microbiology*, **71**, 895-911.

Monteiro A., Teixeira G., Lopes C.M., 2013. Comparative leaf micromorphoanatomy of *Vitis vinifera* ssp. *vinifera* (*Vitaceae*) red cultivars. *Ciencia E Tecnica Vitivinicola*, **28**, 19-28.

OIV, 2001. Descriptor list for grape varieties and *Vitis* species: 2nd edition, www.oiv.int.

Palliotti A., Cartechini A., Ferranti F., 2000. Morpho-anatomical and physiological characteristics of primary and lateral shoot leaves of Cabernet Franc and Trebbiano Toscano grapevines under two irradiance regimes. *American Journal of Enology and Viticulture*, **51**, 122-130.

Powell G., Maniar S.P., Pickett J.A., Hardie J., 1999. Aphid responses to non-host epicuticular lipids. *Entomologia Experimentalis et Applicata*, **91**, 115-123.

Riederer M., Schreiber L., 2001. Protecting against water loss: analysis of the barrier properties of plant cuticles. *Journal of Experimental Botany*, **52**, 2023-2032.

Rogiers S.Y., Hardie W.J., Smith J.P., 2011. Stomatal density of grapevine leaves (*Vitis vinifera* L.) responds to soil temperature and atmospheric carbon dioxide. *Australian Journal of Grape and Wine Research*, **17**, 147-152.

Ruinen J., 1961. The phyllosphere: I. An ecologically neglected milieu. *Plant and Soil*, **15**, 81-109.

Santos C., Teixeira G., Monteiro A., 2014. Leaf morphonanatomy of Portuguese autoctones white grapevine cultivars of different geographical origin. *X^th International Terroir Congress*, pp. 103-108.

Smith D.B., Askew S.D., Morris W.H., Shaw D.R., Boyette M., 2000. Droplet size and leaf morphology effects on pesticide spray deposition. *Transactions of the ASAE*, **43**, 255-259.

Stasinopoulos S.J., Fisher P.R., Stone B.A., Stanisich V.A., 1999. Detection of two loci involved in (1-3)-β-glucan (curdlan) biosynthesis by *Agrobacterium* sp. ATCC31749, and comparative sequence analysis of the putative curdlan synthase gene. *Glycobiology*, **9**, 31-41.

Stone B.A., Clarke A.E., 1992. Chemistry and Biology of (1-3)-beta-glucans. La Trobe University Press. Melbourne. 803 p.

Vacher C., Hampe A., Porté A.J., Sauer U., Compant S., Morris C.E., 2016. The phyllosphere: microbial jungle at the plant-climate interface. *Annual Review of Ecology, Evolution, and Systematics*, **47**, 1-24.

Verma D.P.S., Hong Z., 2001. Plant callose synthase complexes. *Plant Molecular Biology*, **47**, 693-701.

Watanabe T., Yamaguchi I., 1991. Evaluation of wettability of plant leaf surfaces. *Journal of Pesticide Science*, **16**, 491-498.